Science of the Total Environment xxx (xxxx) xxx

Contents lists available at ScienceDirect

Science of the Total Environment

journal homepage: www.elsevier.com/locate/scitotenv

Enantioselective toxicity and oxidative stress effects of acetochlor on earthworms (*Eisenia fetida*) by mediating the signaling pathway

Yalei Liu, Kuan Fang, Xiaolian Zhang, Tong Liu *, Xiuguo Wang *

Tobacco Research Institute of Chinese Academy of Agricultural Sciences (CAAS), Qingdao 266101, PR China

HIGHLIGHTS

- The environmental fate of *S*-ACT and *R*-ACT in the soil was monitored.
- *R*-ACT and *S*-ACT induced significant enantioselective toxicity on earthworms.
- *R*-ACT induced stronger stress responses in earthworms by mediating signaling pathways.
- *R*-ACT may have a higher risk to the soil environment than *S*-ACT.

GRAPHICAL ABSTRACT

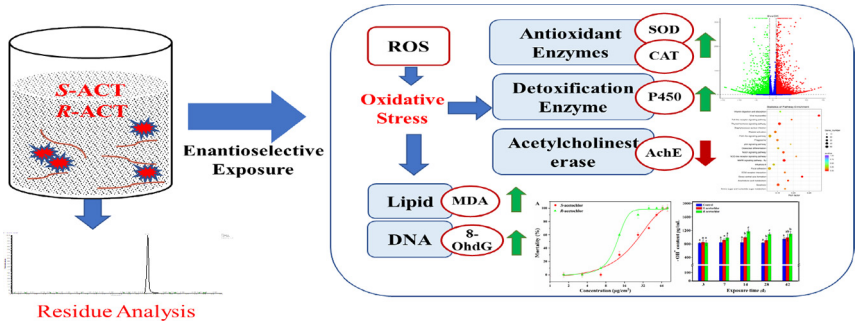

ARTICLE INFO

Article history:
Received 8 August 2020
Received in revised form 21 September 2020
Accepted 23 September 2020
Available online xxxx

Editor: Daqiang Yin

Keywords:
Acetochlor
Enantiomer
Earthworm
Toxicity
Transcriptomic

ABSTRACT

Acetochlor (ACT) as a widely used chiral chloroacetamide herbicide is appropriate to evaluate the potential toxicity in soil ecosystems at enantiomeric level. The acute and subchronic toxicities of *R*-acetochlor (*R*-ACT) and *S*-acetochlor (*S*-ACT) on earthworms (*Eisenia fetida*) were investigated in the present study. Residual analyses showed that *S*-ACT degraded faster than *R*-ACT in artificial soil with half-lives of 16.5 and 21.7 d, respectively. Additionally, significant enantioselective acute toxicity in earthworms from between *S*-ACT and *R*-ACT ($p < 0.05$) was observed, and the acute toxicity of *R*-ACT were 1.9 and 1.5 times higher than those of *S*-ACT in the filter paper test and artificial soil test. The hydroxyl radical ($\bullet OH^-$) content, superoxide dismutase (SOD) and antioxidant enzyme catalase (CAT) activities, and cytochrome P450 content in earthworms significantly increased under the influence of ACT enantiomers; however, the acetylcholinesterase (AchE) activity was significantly inhibited after exposure to the two enantiomers. Moreover, lipid peroxidation and DNA damage were induced by ACT enantiomers. The results of transcriptome sequencing indicated that *R*-ACT induced a stronger oxidative stress effect than *S*-ACT in earthworms by mediating signaling pathways, which may be the primary reason for the enantioselective toxicity between *S*-ACT and *R*-ACT. Overall, the results demonstrated that *R*-ACT has a higher risk than *S*-ACT in the soil environment, which is important for understanding the enantioselective behavior of chloroacetamide pesticides.

1. Introduction

The rapid evolution of populations has accelerated the demand for crop production, resulting in higher rates and amounts of pesticides used to enhance agricultural productivity and crop yields (Zubrod et al., 2019). The current application of herbicides accounts for more than 60% of the total pesticides used in agricultural production (Fathy et al., 2019). Previous research indicated that less than 1% of herbicides reach target weeds, and most herbicides are deposited in the surrounding environment (Pimentel, 1995). Pesticides from multiple sources are released into the environment, resulting in pollution that affects crops, soil, and water, and they may pose health risks to non-target organisms in the environment.

* Corresponding authors.
E-mail addresses: liutong@caas.cn (T. Liu), wangxiuguo@caas.cn (X. Wang).

https://doi.org/10.1016/j.scitotenv.2020.142630
0048-9697/

Acetochlor (ACT), as the most common selective chloroacetamide herbicide, is generally used to control annual grasses and broadleaf weeds in various crops (Li et al., 2016). Its effective weeding effect, wide weed spectrum and moderate price have led it to become one of the three most frequently used herbicides in the global agricultural market; more than 10 million kg of ACT have been used per year since 1977 in China (Li et al., 2016). Some studies have reported that ACT residue concentrations in surface waters are higher than the environmental levels permitted by the United States Environmental Protection Agency and European Union (Chang et al., 2020; Foley et al., 2008). Furthermore, ACT is relatively stable in soil and the degradation half-life can be up to 110 d (Hao et al., 2018; USEPA. United States Environmental Protection Agency, 2004). Sun et al. (2011) detected that ACT concentrations ranged from 0.03 to 709.37 μg/kg in the riparian soils of northeastern China. At the same time, the risk of herbicide transfer was also modeled, showing that ACT was detected in 97% of the samples (Sun et al., 2013). The widespread contamination of ACT may induce adverse effects on organisms in soil environments.

A previous study showed that ACT induced DNA damage in earthworms, and their growth and reproduction decreased significantly after exposure to more than 20 mg/kg of ACT (Xiao et al., 2006a). Additionally, ACT could induce oxidative stress and decreased activities of antioxidative enzymes in the liver of zebrafish (*Danio rerio*) and the human liver carcinoma (HepG2) cell line (Chang et al., 2020; Huang et al., 2020). At the same time, ACT as a chiral compound, has a pair of enantiomers *R*-acetochlor (*R*-ACT) and *S*-acetochlor (*S*-ACT). Due to the chiral structures of nucleic acids, proteins, and sugars, the enantioselective behavior of chiral pollutants is evident in many aspects such as metabolism, absorption or toxicity (Liu et al., 2018). Because of the different behaviors of chiral pesticides in the environment, it is crucial to assess the risk of ACT at the enantiomer level. Xu et al. (2016) found that the enantiomers of ACT exhibited enantioselective behavior in the developmental toxicity and immunotoxicity of zebrafish embryos. Xie et al. (2019) also reported the enantioselective environmental behavior, oxidative stress, and toxin release effect of ACT on harmful cyanobacteria. However, the enantioselective toxicity to non-target organisms in the soil environment remains unclear. Thus, exploring the enantioselective behavior of ACT is crucial in the soil ecosystem.

Earthworms are considered to be the most sensitive biomarkers for soil contamination due to their sensitivity to toxic chemicals (Liu et al., 2018; Ma et al., 2016). Therefore, the acute toxicity, oxidative stress response, and transcriptomic analysis of ACT enantiomers on earthworms (*Eisenia fetida*) were explored in the present study. Moreover, the enantioselective degradation of ACT in soil was also investigated. The results will be helpful for clarifying the enantioselectivity of the environmental safety of ACT in soil ecosystems.

2. Materials and methods

2.1. Materials

R-ACT (99.3% purity) and *S*-ACT (99.3% purity) were separated from their racemate (99.7% purity). The earthworms used in this experiment were *Eisenia fetida* and purchased from a Qingdao ecological farming company (China). The earthworms were acclimated by breeding them in a mixture of sphagnum and cattle feces at 20 ± 2 °C for 14 d prior to testing. Healthy adult earthworms with well-developed clitella and weights of 350 ± 20 mg were selected to test the acute and chronic toxicity. The gut contents in earthworms were removed before the experiment through placing them on moist filter paper for 24 h.

The artificial soil was prepared using the method reported by the Organization for Economic Cooperation and Development (OECD), containing industrial sand (70%), sphagnum peat moss (10%), and kaolin clay (20%), and a pH of 6 ± 0.5 was achieved by adding calcium carbonate ($CaCO_3$) (OECD, 1984).

2.2. Acute toxicity test

The acute toxicity of ACT enantiomers was determined according to the OECD (1984) standard, containing the filter paper contact and artificial soil tests.

The concentration gradients of *R*-ACT and *S*-ACT were 53.1, 39.8, 26.6, 13.3, 6.6 and 3.3 μg/cm^2 (ten for each test solution concentration) in the filter paper contact test. The appropriately sized filter paper was placed in glass tubes (8 × 3 cm) without overlapping. Then, 1 mL of test solution or methanol solution (control) was added to ensure that the filter paper wetted evenly and deionized water (1 mL) was added after the methanol evaporated completely. One gut-cleansed earthworm was placed in each glass tube, which was then sealed with plastic film; air circulation was ensured with breathing holes. The tubes were kept in a dark environment at 20 ± 2 °C; earthworm mortality was determined after 48 h.

For the artificial soil test, the concentration gradients of *R*-ACT and *S*-ACT were 20, 50, 75, 100, 150, and 200 mg/kg (three replicates for each concentration). The test chemicals were added to deionized water and thoroughly mixed with 500 g of artificial soil, and the soil moisture content was regulated to 35% of its dry weight. The samples were transferred to a glass beaker (1 L) containing 10 gut-cleansed earthworms. The samples were kept in a lit environment at 20 ± 2 °C; earthworm mortality was determined after 14 d.

2.3. Subchronic toxicity test

According to the maximum no-observed-effect concentrations observed in the acute toxicity tests, the concentrations of *R*-ACT and *S*-ACT were set at 20 mg/kg (five replicates for each treatment). The test chemicals were sufficiently blended into 750 g of artificial soil. Twenty gut-cleansed earthworms and well-mixed soil were transferred into a glass beaker (1 L). All treatments were subjected to a 12-h light/dark cycle at 20 ± 2 °C. On days 3, 7, 14, 28, and 42, three earthworms and 10 g of soil were randomly picked from each beaker of five replicates to determine various indicators.

2.4. Residue analysis of S-ACT and R-ACT in soil

The test chemicals in soil (5 g) were extracted using deionized water (5 mL) and acetonitrile (20 mL) in a centrifuge tube, which was extracted sufficiently through strongly vortexed at 2500 rpm for 5 min. $MgSO_4$ (4 g) and NaCl (1 g) were added to remove excess water and then centrifuged for 5 min at 4000 rpm. Finally, the sample supernatant was filtered using a 0.22-μm nylon syringe filter.

The effective concentrations of *R*-ACT and *S*-ACT were detected using ultra-performance liquid chromatography tandem mass spectrometry. The chemicals were separated from the tested samples using a Hypersil GOLD C_{18} column (Thermo; 2.1 × 100 mm, 3.0 μm) with a flow rate of 0.25 mL/min and an injection volume of 2.0 μL. Acetonitrile (A) and 0.1% formic acid water (B) were used as the mobile phase, and 0–0.5 min (A/B, 10:90), 1–4 min (A/B, 90:10), and 4.1–5 min (A/B, 10:90) periods were used for the gradient elution program. Positive electrospray ionization (ESI^+) and the multiple reaction monitoring mode (MRM) were used to detect the compound in the sample. In addition, the qualitative ion pair was 270.2/148.1 *m/z* and the quantitative ion pair was 270.2/224.0 m/z, with collision energies of 17 and 10 eV, respectively.

The effectiveness of the analytical method was evaluated using recovery, linearity, limits of quantification (LOQs), and limits of detection (LODs). The linearity of the analytical method was validated by adding *S*-ACT and *R*-ACT solutions to the soil matrix at final concentrations of 0.001, 0.005, 0.01, 0.05, 0.1, 0.5, 1.0, and 5.0 mg/kg. Additionally, the recovery was validated by adding *S*-ACT and *R*-ACT solutions to the blank artificial soil at the additional levels of 0.01, 0.1, and 20 mg/kg. The LODs and LOQs were confirmed at signal-to-noise ratios of 3 and 10. The

results indicated that the residue analysis method of *S*-ACT and *R*-ACT has high accuracy and sensitivity with good linearity and recovery. The specific values are listed in Table S1.

2.5. Measurement of the •OH⁻ content, DNA damage, and detoxifying enzymes

The gut-cleansed earthworms were homogenized in a potassium phosphate buffer (50 mM; w/v:1/10) at a pH of 7.8, and then centrifuged at 8000 ×*g* for 10 min at 4 °C. The sample supernatant was used to determine the hydroxyl radical (•OH⁻) content, 8-hydroxy-2-deoxyguanosine (8-OhdG) content, and cytochrome P450 (CYP450) content.

The •OH⁻ content, 8-OhdG content, and CYP450 content were determined according to the method of Zhang et al. (2020) using a kit obtained from the ShangHai HengYuan Biological Technology Co., Ltd. (Shanghai, China). The •OH⁻ content, 8-OHdG content, and activity of P450 in earthworms were detected by the double antibody sandwich method. The •OH⁻ in earthworms combined with the antibodies of •OH⁻ marked by HRP (Horseradish Peroxidase). Then, 3,3′,5,5′-tetramethylbenzidine (TMB) was added to produce a chromogenic reaction with the compound of antibody-antigen-antibody labeled by the enzyme. The absorbance of the reaction solution was recorded at 450 nm. The detection principle and method of 8-OhdG and CYP450 are the same as those of •OH⁻.

2.6. Measurement of enzyme activities and lipid peroxidation

The acetylcholinesterase (AchE), catalase (CAT), and superoxide dismutase (SOD) activities, as well as malondialdehyde (MDA) content, were determined according to the method of Zhang et al. (2019) using a kit obtained from the Suzhou Comin Biotechnology Co., Ltd. (Suzhou, China). The extraction method of the enzyme solution is the same as that presented in Section 2.5.

One nanomole of TNB (5-mercapto- nitrobenzoic acid) was produced by AchE per minute per milligram of protein, and the amount of AchE was defined as one unit of AchE activity. The sample solution contained 800 μL of buffer ($Na_2HPO_4 \cdot 12H_2O$ and $NaH_2PO_4 \cdot 2H_2O$), 100 μL of enzyme solution, 50 μL of DTNB (5,5′-dithiobis-(2-nitrobenzoic acid)), and 50 μL of acetylcholine chloride. The absorbance of the reaction samples was recorded at 412 nm for 3 min.

One unit of CAT activity was defined as the degradation of 1 μmol of H_2O_2 caused by 1 mg of protein in 1 min. The reaction sample contained 15 μL of enzyme solution, 90 μL of H_2O_2 solution, 300 μL of sodium chloride saturated solution, and 795 μL of ammonium molybdate solution. The absorbance of the reaction sample was recorded at 405 nm.

One unit of SOD activity was defined as the amount of SOD, which caused a photochemical reaction for half of the NBT (nitro-blue tetrazolium). The reaction solution contained 50 μL of enzyme solution, 50 μL of WST-8 solution, 800 μL of working solution (K_2HPO_4, KH_2PO_4, EDTA solution, and xanthine oxidase), and 100 μL hypoxanthine. The reaction sample was thoroughly mixed and allowed to rested for 30 min. The absorbance of the reaction samples was recorded at 450 nm.

The reaction samples were analyzed for their MDA contents contained 0.2 mL of enzyme supernatant and 0.6 mL of TBA (thiobarbituric acid) solution, which were putted in a 95 °C water bath for 30 min. The absorbance of the reaction solution was recorded at 532 nm.

2.7. Transcriptomic analysis

After 42 d, three gut-cleansed earthworms in each treatment were picked randomly for transcriptome analysis. The degradation and contamination of total RNA were monitored on 1% agarose gels. The purity and integrity were assessed using a NanoPhotometer® spectrophotometer (IMPLEN, CA, USA) and an RNA Nano 6000 Assay Kit (Agilent Technologies, CA, USA). A NEBNext®Ultra™ RNA Library Prep Kit (NEB, USA) was used to create the library for transcriptome sequencing. An Illumina HiSeq 4000 platform (Illumina, Inc., San Diego, CA) was used to sequence the qualified library, and paired-end reads were generated. Clean data (clean reads) were obtained by removing reads containing adapters to ensure the quality and reliability of data analysis. Transcriptome assembly was accomplished using Trinity with all parameters set to default. The p-value <0.05 and |log2 (foldchange)| > 1 was set as the threshold for significantly different expressions. Pathway significant enrichment of differentially expressed genes were annotated using the Kyoto Encyclopedia of Genes and Genomes (KEGG) database.

2.8. Data analysis

The dissipation of *S*-ACT and *R*-ACT in artificial soil was simulated by the first-order kinetic equation:

$$C_t = C_0\, e^{-kt}$$

where C_t represents the concentration (mg/kg) of test chemicals at time t (day) in soil, C_0 represents the initial concentration, and k represents the dissipation rate constant. Among them, the k-value was used to calculate the half-life ($DT_{50} = \ln 2/k$).

SPSS 22.0 software (Chicago, USA) was used to conduct data management and analyses, and Origin 8.5 software was used to complete the figures. Date normality was analyzed using Shapiro-Wilk test and the results showed all data followed a normal distribution. The homogeneity of variance was tested using Levine statistic test in SPSS. An analysis of variance was conducted to evaluate discrepancies, and all data were expressed as the mean ± standard deviation (SD). LSD test was performed to analyze significant differences ($p < 0.05$) among the control and exposure treatments.

The transcriptomic sequencing data were uploaded to the sequence read archive (SRA) of the National Center for Biotechnology Information (NCBI) under BioProject accession No. PRJNA663354 (alias: SUB8134403).

3. Results and discussion

3.1. Residue analysis of S-ACT and R-ACT

The concentrations of pollutants should be monitored in the environmental media because the degradation of pollutants is susceptible to photolysis, microorganisms, etc. (Liu et al., 2018). The residue levels

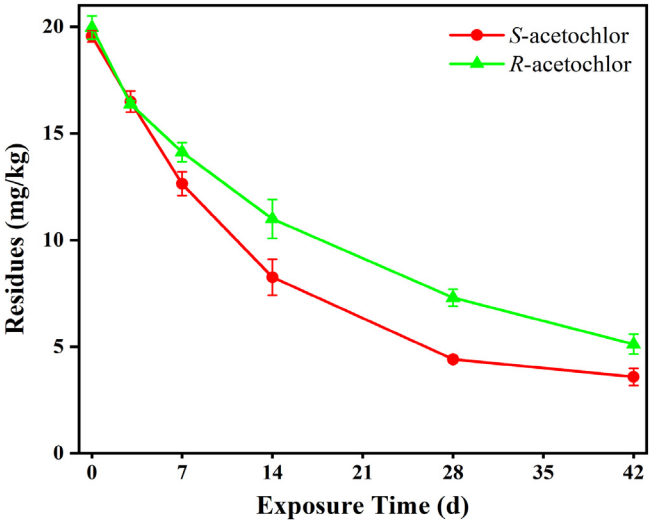

Fig. 1. Residues of *R*-acetochlor and *S*-acetochlor in artificial soil. Data are expressed as the mean ± SD of five replicates.

of *S*-ACT and *R*-ACT in artificial soil were measured, which facilitated the comprehensive risk assessment of ACT in the environment (Fig. 1). The degradation rates of *S*-ACT and *R*-ACT in artificial soil were rather fast, which decreased by 81.7% and 74.6% during the entire exposure period, respectively. Additionally, *S*-ACT and *R*-ACT degradation corresponded to first-order kinetics, and the half-lives were 16.5 and 21.7 d, respectively. Prior study noted that the degradation half-life of ACT in acritical soil was between 9.3 and 15.6 d under laboratory conditions, which is similar to that found in our research (Xiao et al., 2006b). Hao et al. (2018) showed that the degradation of ACT was faster in soil with earthworms than that without earthworms, and the differential dissipation of the enantiomers in the environment is related to various conditions, such as the pH, oxygen, water content, temperature, abundance, and degrading microorganism activity. These results indicate that the residues of *S*-ACT and *R*-ACT decreased rapidly in the artificial soil, and the degradation rate of *S*-ACT was faster than that of *R*-ACT.

3.2. Acute toxicity test results

The results of the acute toxicities of *S*-ACT and *R*-ACT on earthworms were shown in Fig. 2. Earthworm mortality increased as the exposure concentrations of the two chemicals increased. The mortality rate was more prominent in *R*-ACT treatments in the filter paper and artificial soil experiments, which indicated that *S*-ACT and *R*-ACT presented different toxicity levels. The lethal concentrations (LC_{50}) of the contact filter paper test for *S*-ACT and *R*-ACT at 48-h exposure against *E. fetida* were 23.32 and 12.28 μg/cm^2, respectively, and the LC_{50} values of the acute artificial soil test on day 14 were 112.73 and 77.13 mg/kg, respectively. The median lethal concentration of test chemicals on earthworms is an essential indicator for evaluating the toxicity risk to environmental organisms (Prabhakaran et al., 2017). Previous study has shown that the LC_{50} value for ACT on earthworms in artificial soil was 105.5 mg/kg (EFSA. European Food Safety Authority, 2011). The results from Xiao et al. also indicate that ACT has moderate toxic effects on earthworms (Xiao et al., 2006b). Moreover, the results from this experiment indicate that *R*-ACT has stronger toxic effects on earthworms than *S*-ACT.

3.3. Enantioselective behavior and toxicity

Statistical differences in ACT enantioselective degradation and toxicity were shown in Fig. 3. The acute toxicities of the ACT enantiomers showed significant differences in the artificial soil experiment and filter paper experiment ($p < 0.05$). Moreover, the acute toxicity of *R*-ACT was higher in the filter paper and artificial soil experiments, which were 1.9 and 1.5 higher than those of *S*-ACT, respectively. Similar results have also been reported by Xu et al. (2016), who demonstrated that *R*-ACT had stronger effects than *S*-ACT in zebrafish developmental toxicity endpoints. However, the degradation half-lives of *S*-ACT and *R*-ACT in artificial soil showed no significant differences ($p > 0.05$). Previous study has also shown that the degradation of ACT in BG-11 medium was non-enantioselective during the experimental period (Xie et al., 2019). In general, the acute toxicity of ACT to earthworms was enantioselective, but there was no significant difference in its degradation in artificial soil.

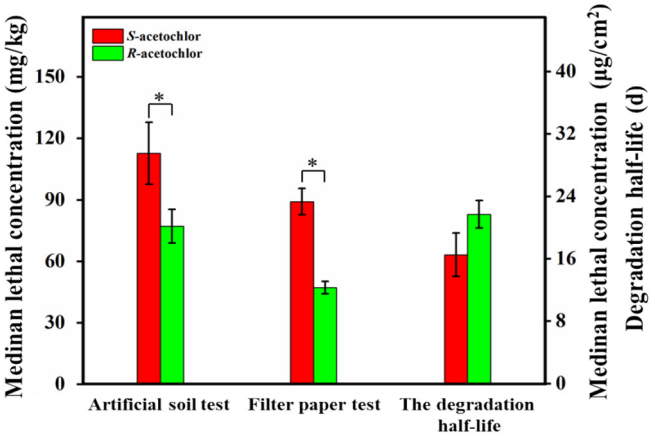

Fig. 3. Statistical analysis of the acute toxicity in the filter paper content test, artificial soil test and degradation half-life in artificial soil (*$p < 0.05$ between treatments).

3.4. Enantioselective effects on •OH$^-$ content in earthworms

Environmental stresses will produce excess reactive oxygen species (ROS), resulting in the response of oxidative stress in organisms (Li et al., 2019). Moreover, •OH$^-$, as an important ROS, can regulate many biological processes in organisms, and is considered to be the most hazardous free radical (Gill and Tuteja, 2010). As shown in Fig. 4, the •OH$^-$ content increased after *S*-ACT and *R*-ACT treatments. No significant differences were observed between the different treatments on days 3 and 7 ($p > 0.05$). Compared with the control group, significant increases were first observed on day 14 ($p < 0.05$), and significant differences were also found between *S*-ACT and *R*-ACT treatments ($p < 0.05$) on days 14 and 28. On day 42, no significant promotion of •OH$^-$ contents was observed between *S*-ACT and control treatments ($p > 0.05$), but significant increases was observed in the *R*-ACT treatment ($p < 0.05$).

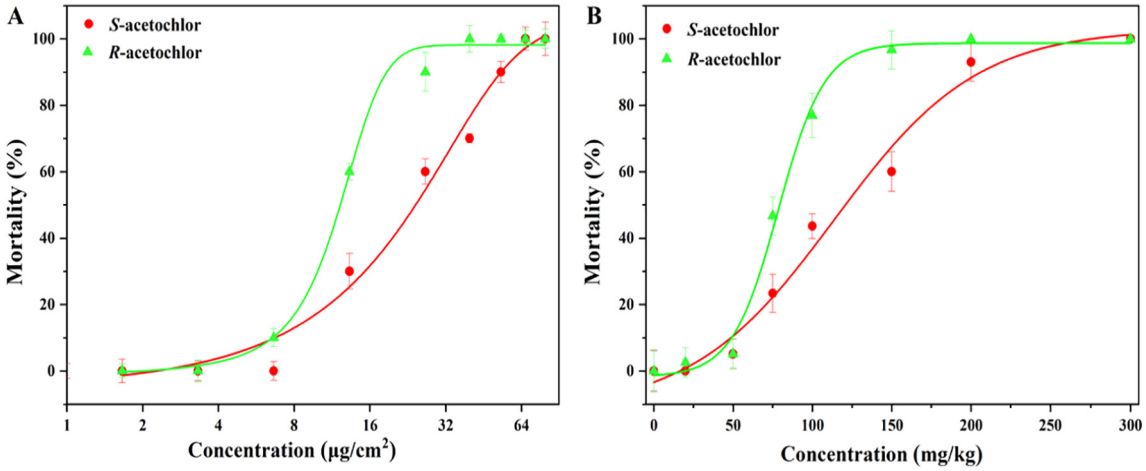

Fig. 2. Dose-effect curves of the contact filter paper test (A) and acute artificial soil test (B) after exposure to *S*-acetochlor and *R*-acetochlor.

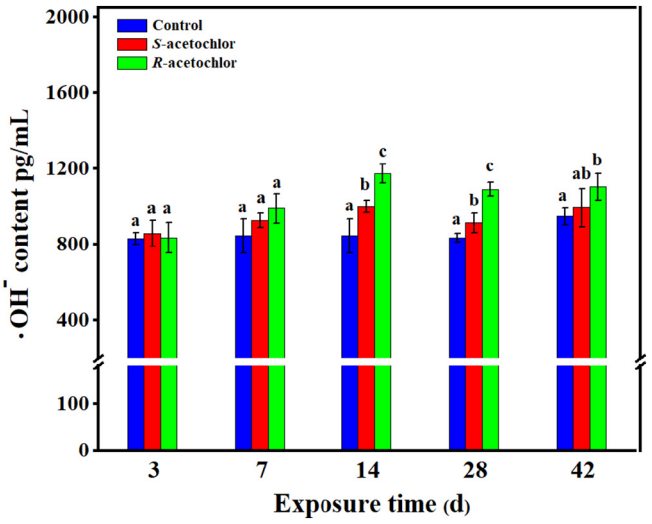

Fig. 4. Effects of *R*-acetochlor and *S*-acetochlor on the •OH$^-$ content in earthworms. Bars are the means ± SD of five replicates. Different letters indicate significant differences ($p < 0.05$) among treatments.

These results suggest that the oxidative stress reaction did not occur at the early stage of exposure. In addition, the •OH$^-$ content in earthworms was more impressionable after *R*-ACT exposure. It has been reported that ACT significantly increased cellular ROS generation and induced oxidative damage responses in the human liver carcinoma (HepG2) cell line (Huang et al., 2020). Oxidative stress response also occurs in zebrafish after ACT treatment (Chang et al., 2020). Therefore, the change in the •OH$^-$ content indicates that ACT caused oxidative stress, and *R*-ACT incited stronger effects than *S*-ACT in earthworms.

3.5. Enantioselective effects on enzyme activities

Damage from oxidative stress is an important toxicity mechanism that occurs because of various pollutants, and the antioxidant defense system is an important way for organisms to protect themselves from oxidative damage (Li et al., 2019; Shao et al., 2019). SOD and CAT are considered to be significant antioxidant enzymes that can remove excess ROS and combat oxidative stress in the cells of organisms (Hu et al., 2016; Liu et al., 2018). After *S*-ACT and *R*-ACT exposure, the trends of SOD and CAT activities in earthworms were similar throughout the entire exposure period (Fig. 5A, B). The activities of SOD and CAT in *S*-ACT and *R*-ACT exposure treatments first decreased and then increased with increasing time. SOD activity increased significantly on days 14 and 28 ($p < 0.05$), and significant differences were observed between *S*-ACT and *R*-ACT treatments ($p < 0.05$). On day 42, no significantly enhanced SOD activity was induced by *S*-ACT ($p > 0.05$), but significant increases were observed in *R*-ACT group ($p < 0.05$). For CAT activity, significant increases were first discovered in *R*-ACT treatments on day 7. Additionally, the trend of ACT activity was similar to that of SOD activity from the day 14.

AchE is a key enzyme in the nerve conduction process that terminates nerve impulses by promoting acetylcholine hydrolysis (Singh et al., 2018). The CYP450 is a detoxifying enzyme in the phase I family and that is responsible for the biotransformation of endogenous and exogenous compounds (Jia et al., 2020). The enzyme activities of AchE and the content of CYP450 were measured for assessing the effects of *S*-ACT and *R*-ACT on earthworms (Fig. 5C, D). The activities of AchE in earthworms were initially significantly inhibited by *S*-ACT and *R*-ACT (on day 3; $p < 0.05$), then increased significantly on day 7 ($p < 0.05$). However, the AchE activity was shown significant inhibitory effect on days 14 and 28 ($p < 0.05$). Additionally, the AchE activity returned to the control level, and no significant differences between different treatments were found at the end of the experiment (day 42; $p > 0.05$). In contrast, the content of CYP450 significantly increased in earthworms after exposure to the two enantiomers. Compared with that of the control group, the CYP450 content in the *S*-ACT and *R*-ACT treatments increased significantly from day 7 ($p < 0.05$), and was highest on the 28th day. Moreover, the activities of AchE and the content of CYP450 in earthworms were more impressionable in *R*-ACT treatment than those in *S*-ACT.

These results demonstrated that ACT exposure can cause oxidative damage to earthworms. The activities of SOD and CAT in earthworms significantly increased to protect themselves from oxidative damage. Compared with *S*-ACT treatments, *R*-ACT induced a greater increase in ROS content, resulting in higher activities of SOD and CAT. Meanwhile, the effects of S-ACT and R-ACT on AchE activity in earthworms first decreased, then increased, and then decreased again. The activation of AChE activity promotes the hydrolysis of neurotransmitters, thereby interrupting the transmission of acetylcholine. Additionally, the inhibition of AChE activity may lead to excessive accumulation of acetylcholine and induce toxic reactions in earthworms. Moreover, the content of CYP450 significantly increased, indicating that CYP450 may play an important role in the metabolism of ACT in earthworms. The effects of *S*-ACT and *R*-ACT on SOD, CAT, AchE and CYP450 were significantly reduced on days 42. This may have occurred because the concentrations of ACT enantiomers were significantly lower at the end of this period. Importantly, the different trends of enzyme activities due to the test chemicals indicated that *S*-ACT and *R*-ACT exhibited selective behavior in earthworms. Several reports have also shown a significant increase of enzymes related to oxidative stress such as SOD and CAT after exposure to ACT in earthworms, zebrafish and harmful cyanobacteria (Chang et al., 2020; Xiao et al., 2006a; Xie et al., 2019). CYP450 is considered a significant biomarker for the assessment of compounds (Jia et al., 2020). Furthermore, environmental stresses, such as heavy metal pollution and pesticide residues significantly inhibit AChE activity in earthworms (Frasco et al., 2005; Singh et al., 2018). Thus, the oxidative stress reaction will be produced in earthworms after exposure to ACT, and a stronger oxidative stress reaction was observed in *R*-ACT treatments.

3.6. Enantioselective effects on lipid peroxidation and DNA damage

The excess ROS can damage many biomacromolecules such as proteins, lipids, and nucleic acids, resulting in lipid peroxidation (LPO) and DNA damage in organisms (Inupakutika et al., 2016; Yang et al., 2020). Among them, cellular function can be negatively impacted by LPO, and lipid-derived radicals can be produced, which aggravate the oxidative stress reaction in cells (Liu et al., 2018). Additionally, the MDA content can indirectly represent the level of LPO. The excess ROS, especially the •OH$^-$, also can also induce DNA damage and result in base modification, base deletion, strand breaks, and pyrimidine dimers (Inupakutika et al., 2016). 8-OHdG, which is produced by •OH$^-$ attack on the C_8 of guanine, is considered to be an important indicator of DNA oxidative damage, (Liu et al., 2018).

In this research, the levels of LPO and DNA oxidative damage after exposure to *S*-ACT and *R*-ACT were assessed by measuring the MDA and 8-OHdG contents in earthworms (Fig. 6). The variation trend of MDA content and 8-OHdG content in earthworms were similar after exposed to *S*-ACT and *R*-ACT. Only increased for MDA between days 7 and 14, then was steady. Only increased for 8-OHdG from 3 to 7 days, and then concentrations were relatively steady. In this study, the increased MDA and 8-OHdG contents indicated that *S*-ACT and *R*-ACT induced LPO and DNA oxidative damage in earthworm cells. Additionally, the levels of LPO and DNA damage in earthworms were significantly higher than those in the control group in the later stage of exposure. Moreover, the lipid peroxidation and DNA oxidative damage of earthworms were not reduced by the rapid degradation of ACT enantiomers. This result showed that the contents of ROS after exposure to *S*-ACT and *R*-ACT were over the scavenging capacity of the antioxidant enzymes and

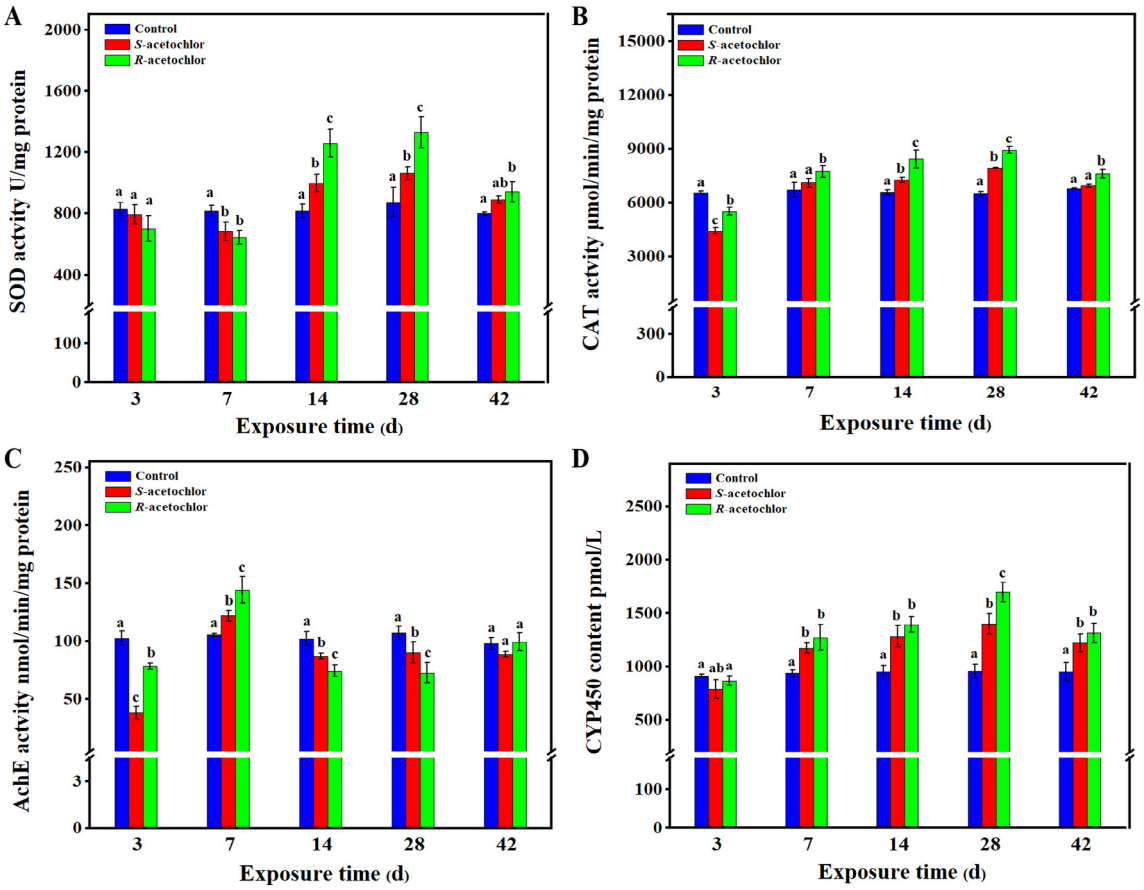

Fig. 5. Effects of *R*-acetochlor and *S*-acetochlor on the SOD activity (A), CAT activity (B), AchE activity (C) and CYP450 content (D) in earthworms. Data are expressed as the mean ± SD of five replicates. Different letters indicate significant differences ($p < 0.05$) among treatments.

resulted in damage to the lipids and DNA in earthworms. This result is in agreement with earlier studies, which demonstrated that the MDA content significantly increased in zebrafish and DNA damage increased in earthworms after exposure to ACT (Chang et al., 2020; Xiao et al., 2006a). Huang et al. (2020) showed that ACT significantly reduced the production of antioxidants and augmented MDA content in HepG2 cells. Furthermore, the accumulation of MDA and DNA-single strand breaks caused by ACT were indicated in *Bufo raddei* tadpoles (Liu et al., 2006).

3.7. Transcriptome sequencing analysis of Enantioselective toxic effects

Transcriptome analysis, as a powerful tool for analyzing the expression level of mRNA, is widely used to assess the risk of pollutants on organisms in the environment (Chai et al., 2020; Mkhinini et al., 2019). The differentially expressed genes (DEGs) in earthworms affected by *S*-ACT and *R*-ACT compared to the control group are shown in Fig. 7A. The volcano plot visually shows that 11,256 DEGs were detected in earthworms after exposure to *S*-ACT, while 15,465 DEGs were detected

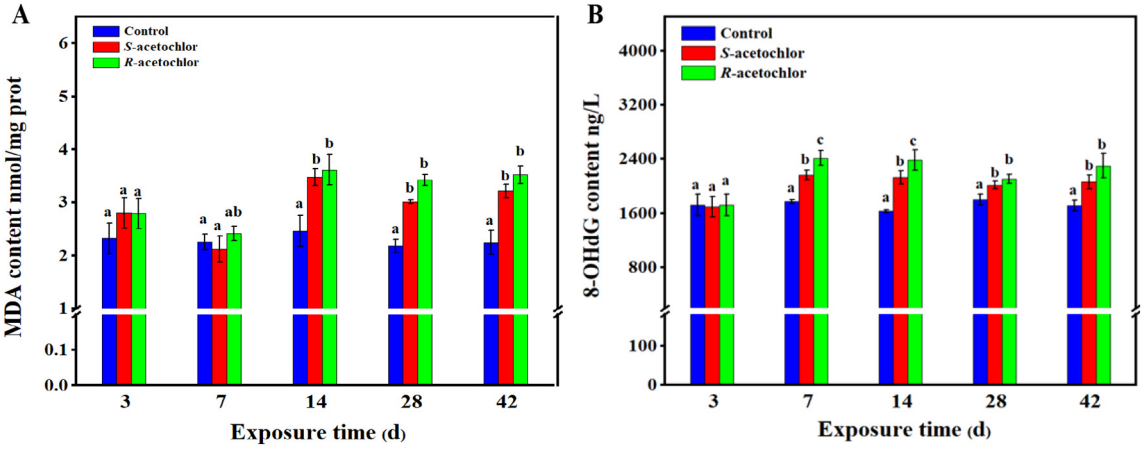

Fig. 6. Effects of *R*-acetochlor and *S*-acetochlor on the MDA content (A) and 8-OHdG content (B) in earthworms. Data are expressed as the mean ± SD of five replicates. Different letters indicate significant differences ($p < 0.05$) among treatments.

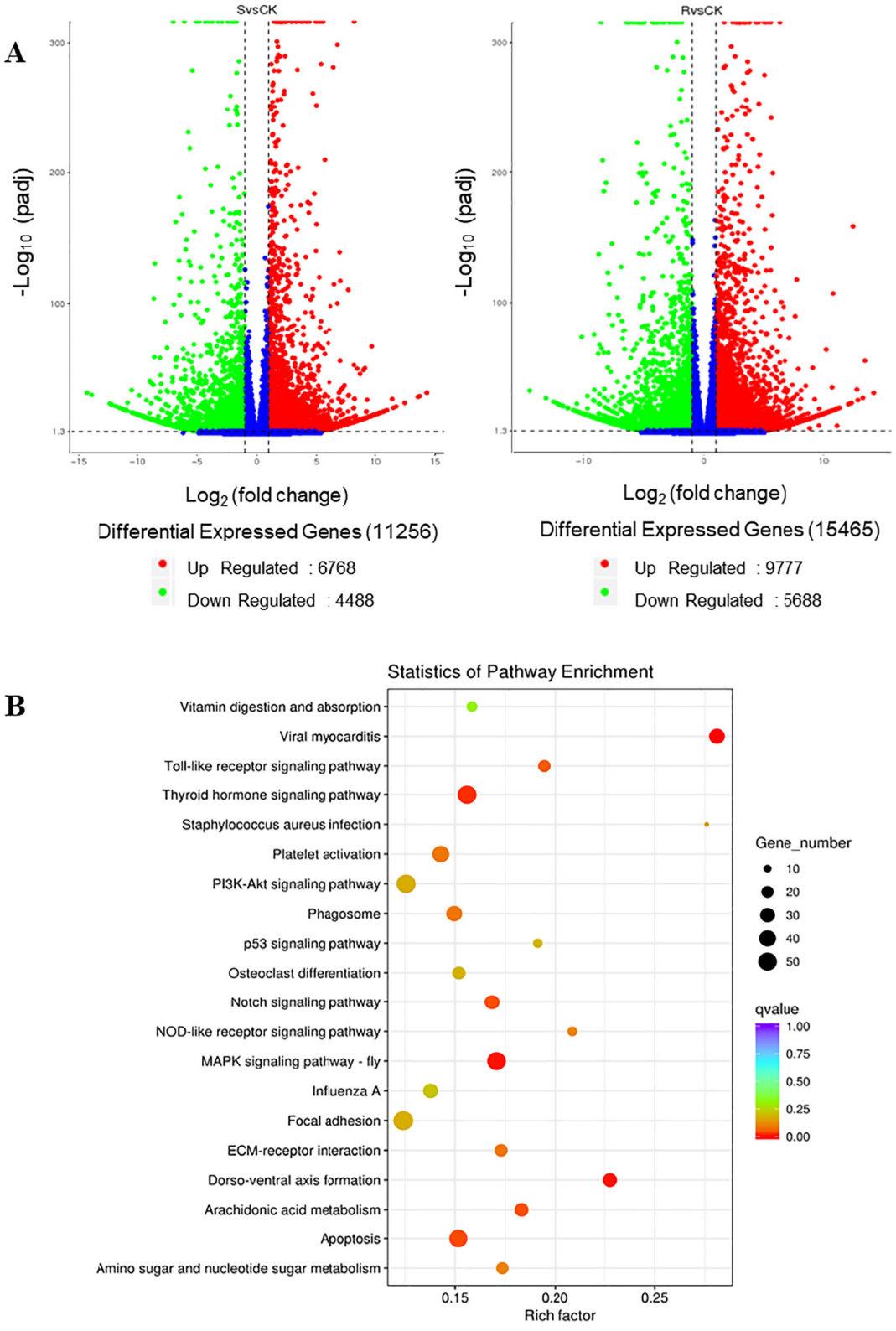

Fig. 7. Volcano plot of DEGs after exposure to *R*-acetochlor and *S*-acetochlor compared with the control group (A) and function annotation of DEGs between *R*-acetochlor and *S*-acetochlor using the KEGG database (B).

in the *R*-ACT treatment. The number of DEGs in earthworms treated with *R*-ACT was significantly higher than that of the *S*-ACT treatment. Among these results, a total of 6788 and 9777 upregulated genes were found in earthworms after *S*-ACT and *R*-ACT exposure, respectively. Additionally, the numbers of downregulated genes in earthworms affected by *S*-ACT and *R*-ACT were 4488 and 5688, respectively. Previous research reported that differences in gene expression and mRNA expression in earthworms were significantly affected by pesticide residues and heavy metals (Chai et al., 2020; Liu et al., 2018). Moreover, the level of protein expression in zebrafish was shown to significantly increase after *R*-ACT exposure compared with that after *S*-ACT exposure (Xu et al., 2016). This study revealed that the expression levels of mRNA in

earthworms were significantly affected by *S*-ACT and *R*-ACT, and *R*-ACT had a stronger influence than *S*-ACT.

Furthermore, KEGG pathway enrichment analysis was performed to further evaluate the biological significance of DEGs. As shown in Fig. 7B, 20 significantly enriched pathways in earthworms after exposure to *S*-ACT and *R*-ACT were listed, and a total of 7 signaling pathways were seriously influenced. Signaling pathways regulate biochemical reactions in cells by molecular signaling, including the regulation of gene expression, change in enzyme activity, bone architecture, and DNA synthesis. The amount of DEGs and degree of enrichment in the thyroid hormone signaling pathway were higher than those in other signaling pathways. It has been reported that the mRNA expression and thyroid hormone levels in zebrafish larvae were altered by ACT exposure, and *S*-ACT had a stronger thyroid disruptive effect (Xu et al., 2019; Yang et al., 2015). Moreover, the MAPK signaling pathway has also been observed to be seriously influenced, which can cause cell proliferation, differentiation, apoptosis, stress, and other biochemical reactions (Zhong et al., 2020). In this study, the oxidative stress response and oxidative damage were caused by ACT in earthworms, possibly because the function of the signaling pathway was influenced.

Moreover, significant enrichment of the apoptosis pathway indicates that ACT treatment resulted in apoptosis in earthworm cells. In addition, one of the key characteristics of apoptosis was DNA fragmentation, and DNA oxidative damage caused by *S*-ACT and *R*-ACT was proven in this research. Lapied et al. (2011) reported that a TiO_2 nanocomposite induced apoptosis in earthworms; similarly, Chai et al. (2020) reported that DEGs were mainly enriched in the apoptosis pathways in earthworms after exposure to cadmium. This indicates that the enhanced frequency of apoptosis can be used as a sensitive endpoint for assessing adverse effects in many organisms. Furthermore, focal adhesion is an important structure in the cytoskeleton that helps maintain the structural integrity and function (Eke and Cordes, 2015). The unusual function of focal adhesion could induce cellular damage, bring about an imbalance of various enzymes, and the growth inhibition of earthworms. The transcriptome analysis results indicated that the dysfunction of physiological functions in earthworms were disrupted by mediated signaling pathway and apoptosis pathway, resulting in apoptosis, oxidative damage, and changes in enzymatic activity in cells. *R*-ACT may have had a stronger influence on the pathways, which might be the primary reason for the enantioselectivity between the *S*-ACT and *R*-ACT.

4. Conclusion

Biochemical toxicity and genotoxicity in earthworms exposed to *S*-ACT and *R*-ACT were exhibited in the present study. Moreover, enantioselective dissipation of ACT was observed in the artificial soil, and *S*-ACT degraded faster than *R*-ACT. Additionally, the present study suggested that the ACT induced enantioselectivity with regards to the acute toxicity, and the acute toxicity of *R*-ACT were 1.9 and 1.5 times higher those of *S*-ACT in the filter paper content test and artificial soil test. Furthermore, stronger oxidative stress effects were caused by the two enantiomers in later stages of exposure the increase of $\bullet OH^-$ content. The antioxidant and detoxification enzyme activities increased to remove excess ROS in the cells of organisms. Importantly, *R*-ACT led to a stronger oxidative stress response than *S*-ACT, resulting in more serious lipid peroxidation and DNA oxidative damage. The results of transcriptome sequencing indicated that *R*-ACT induced a higher toxicity in earthworms than *S*-ACT by mediating signaling pathways, which may be the primary reason for the enantioselectivity between the *S*-ACT and *R*-ACT. This research is the first comprehensive investigation of the environmental risk of ACT on earthworms at enantiomeric levels. This research investigated the risk of ACT comprehensively from the enantiomeric levels, which is important for the proper use of chloroacetamide herbicide.

Supplementary data to this article can be found online at https://doi.org/10.1016/j.scitotenv.2020.142630.

CRediT authorship contribution statement

Yalei Liu: Data curation, Writing - original draft, Investigation. **Kuan Fang:** Investigation. **Xiaolian Zhang:** Investigation. **Tong Liu:** Conceptualization, Data curation, Writing - review & editing, Project administration, Funding acquisition. **Xiuguo Wang:** Conceptualization, Supervision, Funding acquisition.

Declaration of competing interest

The authors declare that they have no known competing financial interests or personal relationships that could have appeared to influence the work reported in this paper.

Acknowledgments

The present study was supported by grants from the Shandong Provincial Natural Science Foundation (No. ZR201702170228) and the Science Foundation for Young Scholars of the Tobacco Research Institute of Chinese Academy of Agricultural Sciences (No. 2019B01).

References

Chai, L., Yang, Y., Yang, H., Zhao, Y., Wang, H., 2020. Transcriptome analysis of genes expressed in the earthworm *Eisenia fetida* in response to cadmium exposure. Chemosphere 240, 124902.

Chang, Y., Mao, L., Zhang, L., Zhang, Y., Jiang, H., 2020. Combined toxicity of imidacloprid, acetochlor, and tebuconazole to zebrafish (*Danio rerio*): acute toxicity and hepatotoxicity assessment. Environ. Sci. Pollut. Res. 27, 10286–10295.

EFSA. European Food Safety Authority, 2011. Conclusion on the peer review of the pesticide risk assessment of the active substance acetochlor. EFSA J. 9, 2143. https://efsa.onlinelibrary.wiley.com/doi/epdf/10.2903/j.efsa.2011.2143.

Eke, I., Cordes, N., 2015. Focal adhesion signaling and therapy resistance in cancer. Semin. Cancer Biol. 31, 65–75.

Fathy, M., Mohamed, I.A., Farghal, A.I., Temerak, S.A., Sayed, A.E., 2019. Hemotoxic effects of some herbicides on juvenile of nile tilapia *Oreochromis niloticus*. Environ. Sci. Pollut. Res. 26, 30857–30865.

Foley, M.E., Sigler, V., Gruden, C.L., 2008. A multiphasic characterization of the impact of the herbicide acetochlor on freshwater bacterial communities. ISME. J. 2, 56–66.

Frasco, M.F., Fournier, D., Carvalho, F., Guilhermino, L., 2005. Do metals inhibit acetylcholinesterase (AchE) implementation of assay conditions for the use of AchE activity as a biomarker of metal toxicity. Biomarkers 10, 360–375.

Gill, S.S., Tuteja, N., 2010. Reactive oxygen species and antioxidant machinery in abiotic stress tolerance in crop plants. Plant Physiol. Biochem. 48, 909–930.

Hao, Y., Zhao, L., Sun, Y., Li, X., Weng, L., Xu, H., Li, Y., 2018. Enhancement effect of earthworm (*eisenia fetida*) on acetochlor biodegradation in soil and possible mechanisms. Environ. Pollut. 242, 728–737.

Hu, S., Zhang, W., Li, J., Lin, K., Ji, R., 2016. Antioxidant and gene expression responses of *Eisenia fetida* following repeated exposure to BDE209 and Pb in a soil-earthworm system. Sci. Total Environ. 556, 163–168.

Huang, T., Huang, Y., Huang, Y., Yang, Y., Zhao, Y., Martyniuk, C., 2020. Toxicity assessment of the herbicide acetochlor in the human liver carcinoma (HepG2) cell line. Chemosphere 243, 125345.

Inupakutika, M.A., Sengupta, S., Devireddy, A.R., Azad, R.K., Mittler, R., 2016. The evolution of reactive oxygen species metabolism. J. Exp. Bot. 67, 5933–5943.

Jia, Z., Zhang, Y., Huang, Q., Jones, A., Zhao, C., 2020. Acute toxicity, bioconcentration, elimination, action mode and detoxification metabolism of broflanilide in zebrafish, *Danio rerio*. J. Hazard. Mater. 394, 122521.

Lapied, E., Nahmani, J.Y., Moudilou, E., Chaurand, P., Labille, J., Rose, J., Exbrayat, J.M., Oughton, D., Joner, E., 2011. Ecotoxicological effects of an aged tio-2 nanocomposite measured as apoptosis in the anecic earthworm *lumbricus terrestris* after exposure through water, food and soil. Environ. Int.37, 1105-1110.

Li, L., Wang, M., Chen, S., Zhao, W., Zhao, Y., Wang, X., Zhang, Y., 2016. A urinary metabonomics analysis of long-term effect of acetochlor exposure on rats by ultra-performance liquid chromatography/mass spectrometry. Pestic. Biochem. Physiol. 128, 82–88.

Li, M., Xu, G., Yu, R., Wang, Y., Yu, Y., 2019. Bioaccumulation and toxicity of pentachloronitrobenzene to earthworm (*Eisenia fetida*). Ecotoxicol. Environ. Saf. 174, 429–434.

Liu, Y., Zhang, Y., Liu, H., Huang, D., 2006. The role of reactive oxygen species in the herbicide acetochlor-induced dna damage on *bufo raddei* tadpole liver. Aquat. Toxicol. 78, 21–26.

Liu, T., Chen, D., Li, Y., Wang, X., Wang, F., 2018. Enantioselective bioaccumulation and toxicity of the neonicotinoid insecticide dinotefuran in the earthworms (*eisenia fetida*). J. Agric. Food Chem. 66, 4531–4540.

Ma, T., Chen, L., Wu, L., Zhang, H., Luo, Y., 2016. Oxidative stress, cytotoxicity and genotoxicity in earthworm *Eisenia fetida* at different Di-*n*-butyl phthalate exposure levels. PLoS One 11, e0151128.

Mkhinini, M., Boughattas, I., Bousserhine, N., Banni, M., 2019. Biochemical and transcriptomic response of earthworms *Eisenia andrei* exposed to soils irrigated with treated wastewater. Environ. Sci. Pollut. Res. 26, 2851–2863.

Organization for economic co-operation and development, test 207: earthworm, acute toxicity tests. In: OECD (Ed.), OECD Guidelines for Testing of Chemicals. OECD, Paris, France.

Pimentel, D., 1995. Amounts of pesticides reaching target pests: environmental impacts and ethics. J. Agric. Environ. Ethics 8, 17–29.

Prabhakaran, V.S., Sengottayan, S.N., Athirstam, P., Annamalai, T., Muthiah, C., Edwin, E.S., Selvaraj, S.R., Kandaswamy, K., Wayne, B.H., Veeramuthu, D., Naif, A.A., 2017. Acute toxicity of chemical pesticides and plant-derived essential oil on the behavior and development of earthworms, *Eudrilus eugeniae* (Kinberg) and *Eisenia fetida* (Savigny). Environ. Sci. Pollut. Res. 25, 10371–10382.

Shao, Y., Hou, K., Du, Z., Li, B., Wang, J., Juhasz, A.L., Zhu, L., 2019. Evaluation of the toxicity of 1-butyl-3-methyl imidazolium tetrafluoroborate using earthworms (*Eisenia fetida*) in two soils. Sci. Total Environ. 686, 946–958.

Singh, S., Tiwari, R.K., Pandey, R.S., 2018. Evaluation of acute toxicity of triazophos and deltamethrin and their inhibitory effect on ache activity in *channa punctatus*. Toxicol. Rep. 5, 85–89.

Sun, X., Zhou, Q., Ren, W., Li, X., Ren, L., 2011. Spatial and temporal distribution of acetochlor in sediments and riparian soils of the Songhua River Basin in northeastern China. J. Environ. Sci. 23, 1684–1690.

Sun, X., Zhou, Q., Ren, W., 2013. Herbicide occurrence in riparian soils and its transporting risk in the songhua river basin, China. Agron. Sustain. Dev. 33, 777–785.

USEPA. United States Environmental Protection Agency, 2004. Drinking Water Exposure Assessment for Acetochlor. Office of Prevetion, Pesticides and Toxic Substances (No. December 30, 11).

Xiao, N., Song, Y., Ge, F., Signaling, X., Ou-Yang, Z., 2006a. Biomarkers responses of the earthworm *Eisenia fetida* to acetochlor exposure in OECD soil. Chemosphere. 65, 907–912.

Xiao, N., Jing, B., Ge, F., Liu, X., 2006b. The fate of herbicide acetochlor and its toxicity to *Eisenia fetida* under laboratory conditions. Chemosphere. 62, 1366–1373.

Xie, J., Zhao, L., Liu, K., Liu, W., 2019. Enantiomeric environmental behavior, oxidative stress and toxin release of harmful cyanobacteria *Microcystis aeruginosa* in response to napropamide and acetochlor. Environ. Pollut. 246, 728–733.

Xu, C., Tu, W., Deng, M., Jin, Y., Lu, B., Zhang, C., Lin, C., Wu, Y., Liu, W., 2016. Stereoselective induction of developmental toxicity and immunotoxicity by acetochlor in the early life stage of zebrafish. Chemosphere 164, 618–626.

Xu, C., Sun, X., Niu, L., Yang, W., Tu, W., Lu, L., Song, S., Liu, W., 2019. Enantioselective thyroid disruption in zebrafish embryo-larvae via exposure to environmental concentrations of the chloroacetamide herbicide acetochlor. Sci. Total Environ. 653, 1140–1148.

Yang, M., Hu, J., Li, S., Ma, Y., Zhu, G., 2015. Thyroid endocrine disruption of acetochlor on zebrafish (*Danio rerio*) larvae. J. Appl. Toxicol. 36, 844–852.

Yang, X., Li, Y., Wang, X., 2020. Effects of ciprofloxacin exposure on the earthworm *Eisenia fetida*. Environ. Pollut. 262, 114287.

Zhang, S., Ding, J., Razanajatovo, R.M., Jiang, H., Zou, H., Zhu, W., 2019. Interactive effects of polystyrene microplastics and roxithromycin on bioaccumulation and biochemical status in the freshwater fish red tilapia *(oreochromis niloticus)*. Sci. Total Environ. 648, 1431–1439.

Zhang, C., Zhou, T., Du, Z., Albert, J., Zhu, L., Wang, J., Wang, J., Li, B., 2020. Applying fungicide on earthworms: biochemical effects of *Eisenia fetida* exposed to fluoxastrobin in three natural soils. Environ. Pollut. 258, 113666.

Zhong, J., Wang, Z., Xie, Q., Li, T., Chen, K., Zhu, T., Tang, Q., Shen, C., Zhu, J., 2020. Shikonin ameliorates D-galactose-induced oxidative stress and cognitive impairment in mice via the MAPK and nuclear factor-κB signaling pathway. Int. Immunopharmacol. 83, 106491.

Zubrod, J.P., Bundschuh, M., Arts, G., Bruhl, C.A., Imfeld, G., Knabel, A., Payraudeau, S., Rasmussen, J.J., Rohr, J., Scharmuller, A., Smalling, K., Stehle, S., Schulz, R., Schafer, R.B., 2019. Fungicides: an overlooked pesticide class? Environ. Sci. Technol. 53, 3347–3365.